https://doi.org/10.2352/ISSN.2470-1173.2020.7.ISS-213

Calibration Empowered Minimalistic Multi-Exposure Image Processing Technique for Camera Linear Dynamic Range Extension

Nabeel. A. Riza and Nazim Ashraf; School of Engineering, University College Cork; Cork, Ireland

Abstract

Proposed for the first time is a novel calibration empowered minimalistic multi-exposure image processing technique using measured sensor pixel voltage output and exposure time factor limits for robust camera linear dynamic range extension. The technique exploits the best linear response region of an overall non-linear response image sensor to robustly recover via minimal count multi-exposure image fusion, the true and precise scaled High Dynamic Range (HDR) irradiance map. CMOS sensor-based experiments using a measured Low Dynamic Range (LDR) 44 dB linear region for the technique with a minimum of 2 multi-exposure images provides robust recovery of 78 dB HDR low contrast highly calibrated test targets.

Introduction

Many natural and human-made scenes have naturally high (e.g., > 120 dB) dynamic range (DR), i.e., bright light pixel to weak light pixel irradiance ratios exceeding one million to one [1-2].

Apart from the HDR nature, many scenes can also have critical low contrast regions within the full HDR. Today, many systems across diverse applications are emerging with semi-autonomous (i.e., part human and part machine) and fully autonomous (i.e., all machine) control that rely on image sensor data to make critical operational decisions. Fundamentally, unreliable image data provided to these machines delivers unreliable system decisions. Thus, an image sensor must provide the highest reliability image data possible within the scene HDR, keeping in mind that low contrast regions are accurately measured.

In the visible light region, silicon CMOS image sensor technology [3] is the workhorse sensor for today's camera systems. Most commonly available and deployed CMOS sensors have limited (e.g., 60 dB to 80 dB) dynamic ranges and over the years extensive design and microelectronics fabrication work has been conducted to realize HDR CMOS sensors [4] such as 140 dB all-logarithm response sensors [5]. Given most white light CCD/CMOS sensors have limited DR performance making them LDR sensors, a common approach used to generate HDR images from an LDR sensor is to capture multiple LDR images by using different exposures of the camera and then engaging image fusion to compute an HDR image. Although this approach has been known since 1853 for negative-positive photography by E. Baldus [1] and via special exposure sensitive films as proposed by C. W. Wyckoff in 1962 [6], the proposal to use an electronic image sensor (e.g., CCD) for taking multiple exposure images was first put forth in 1982 by Sony Corp. [7] and independently by P. J. Burt in 1984 [8] and later by Polaroid Corp. in 1987 [9]. Image processing methods to achieve HDR using LDR device images with varying exposures took off in 1993 by works of S. Mann [10] and P. J. Burt and R. J. Kolczynski [11].

Since then, the field of HDR image processing and devices based on the multiple exposures LDR-to-HDR method has produced many works that have used both complex sensor design hardware solutions [12-13] plus advanced image processing mathematics and computational algorithms [14-19], including matrix rank minimization techniques [20-21] to try to achieve the goal of "true" observed scene HDR recovery. A survey of early and recent prior works [14-17, 20-25], indicates that multi-image processing HDR scene recovery methods use the camera's observed multiple exposure LDR scenes to generate the camera's input-output response function. Specifically, the LDR camera is pointed to real-life scenes to generate a large image data set that undergoes specific mathematical transformations via algorithmic computational processing to arrive at a synthesized Camera Response Function (CRF). This estimated CRF is then used in the HDR recovery of unknown observed scenes via custom processing of several captured LDR scenes.

Furthermore, in some prior works, computer synthesized scenes from an LDR data set were used to estimate the CRF [21], although some early works used non-HDR and limited irradiance step resolution Macbeth test charts (they have different color patches with different transmission) for color calibration [26]. Such methods seem counter intuitive to achieving a robust and "true" scene scaled irradiance map HDR recovery given the camera only observes scenes with unknown irradiances or the camera has not physically produced the image data set used for CRF generation as these images were synthesized. As such, one cannot logically expect reliable and "true" HDR image recovery via multi-image processing using the said CRF.

The present paper takes on this challenge by proposing a true physical calibration empowered minimalistic computations multi-exposure image processing technique for camera linear dynamic range extension enabling HDR low contrast image recovery.

Calibration empowered minimalistic multi-exposure image processing

There are some fundamentals described next that are the basis of the proposed calibration empowered minimalistic multi-exposure image processing technique that uses LDR images to recover an HDR image.

1. For a given scene pixel incident irradiance value I_i, increasing photo-sensor pixel exposure time T_e gives proportionally more total photons N_i incident on the photo-sensitive area A_p pixel bucket, i.e., there is a ***fundamental linear relationship between N_i and T_e***, i.e., $N_i=(I_i\ T_e\ A_p)/E_p$ where E_p is the photon energy. Hence camera images taken with different T_e values have N_i values that are ideally linearly proportional to their T_e values. This makes multi-exposure image processing a fundamentally linear image transformation for an ideal camera.

2. More absorbed photons in the pixel generate more photo-electrons in the pixel readout electronic circuit giving an output photo-voltage $v_p = \eta\ C(N_i)\ N_i$, where $\eta < 1$ is the quantum efficiency (i.e., photons to electrons conversion factor) and $C(N_i)$ is a photosensor pixel device & circuit design specific parameter that

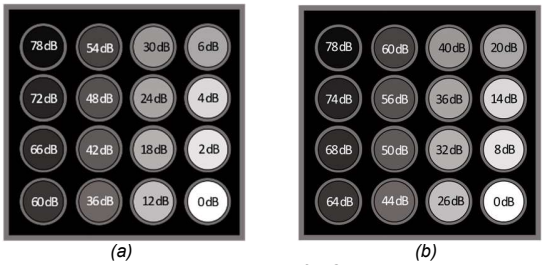

(a) (b)

Figure 1. *(a) The 78 dB target design used for CRF calibration. (b) A different 78 dB target design used for the LDR to HDR multi-image test.*

is a function of N_i. In other words, depending on the photon count N_i experienced by the pixel during its exposure time, the pixel output voltage v_p gets a specific weight. One can rewrite the sensor pixel output voltage as $v_p = K\, C(N_i)\, I_i T_e$ where $K = (\eta A_p)/E_p$ is a constant. It is very important to note that in real physical optical sensors, $C(N_i)$ is not a constant which means that ***in real sensors, v_p and incident N_i (and thus the product I_iT_e) do not have a perfectly linear relationship*** and in fact tend to have a non-linear or at best, pseudo-linear behavior when designing CMOS/CCD/FPA sensors and in particular, HDR sensors. In other words for a fixed T_e, v_p varies linearly with changing I_i for a limited I_i range between I_{max} and I_{min}. Similarly for a fixed I_i, v_p varies linearly with changing T_e for a limited T_e range increasing from T_1 to T_n where $T_n = P_{max} T_1$ and P_{max} is the maximum exposure time factor. Thus to find the true incident I_i (or true scaled irradiance I_s), one must experimentally operate within this linear T_e and I_i limit. Therefore, one must find $C(N_i)$ within these limits using known I_i values via a calibrated test target over the chosen design HDR_D value. In this case, K and $T_e = T_c$ used in the experiment are known quantities. K is constant independent of $C(N_i)$ that depends on the chosen optical band (e.g., average photon energy E_p within a band), pixel area, and photo-sensitive material. Defining v_p as the camera system output and I_s as the camera system scaled input irradiance where $I_i = \alpha I_s$, where α is an introduced scaling constant, one can define the CRF by the input/output equation $v_p = mI_s + d$ where $m = \alpha K T_c C(N_i)$ and d is an offset constant. Because $C(N_i)$ is in practice not a constant over the full HDR_D range of I_i values for a given T_e, the CRF is fundamentally nonlinear. One assumes all photo-sensitive pixels in an array sensor have the same CRF.

3. Reliable low contrast scaled irradiance image detection over the HDR_D requires a linear CRF with a fixed slope, i.e., m is fixed. Specifically, m should equal 1 as then for a scaled input irradiance I_s (unitless) that for example varies from 1 to 10,000, the sensor signal output v_p (unitless) also varies from 1 to 10,000, thus allowing low contrast detection over the entire HDR_D, in this case, 80 dB camera dynamic range. Moreover, with m=1, the input irradiances are not read as compressed sensor outputs (slope <1) that create smaller output voltage steps that are harder to detect given electronic noise limits. On the other hand with slope >1, one gets stretched voltage outputs that makes inefficient use of the output voltage maximum limit leading to a lower detected camera dynamic range. A critical HDR test for low contrast image detection is the reliable recovery of a low contrast, i.e., 2:1 irradiance step between pixels or 6 dB dynamic range differential over the full HDR_D [27]. Given this 6 dB step irradiance detection requirement and that most monotonically increasing CRF functions have some linear sub-region, the defined slope m=1 region that is intrinsically an ideal linear region of a CRF must be determined using the experimentally found $C(N_i)$ data. With the slope m nearest to 1 sub-region of the CRF found, also measured for this region are the v_p maximum and minimum values v_{max} and v_{min}, respectively. Hence determined is the experimental LDR value called $\mathbf{LDR_E\ (dB) = 20\ log\ (v_{max}/v_{min})}$ of this restricted critical near linear region of the deployed overall non-linear response photo-sensor.

4. Use of multi-exposure image processing (which is a linear process as explained earlier) with the experimentally determined linear sub-zone CRF of the deployed camera most importantly keeps the overall HDR camera system linear, thus preserving the low contrast image detection feature over the HDR_D, a mission of the proposed technique. In addition, operating a camera system within the controlled bounds of linearity, i.e., only experimental sensor provided data between v_{max} and v_{min} is used for computational HDR imaging minimizes the emergence of non-linearity created image artifacts. Given a desired HDR_D value, one must satisfy $\mathbf{N \times LDR_E > HDR_D}$, where N is an integer and is the number of multi-exposure LDR images experimentally captured by the designed camera system. To process all N>1 acquired image data v_p values using the same irradiance scaling, each v_p value for the n^{th} image (n>1) must be divided by its exposure time factor P_n. The n^{th} exposure time is given by $\mathbf{T_n = P_n T_1}$ with P_n>1 and n>1 with T_n referenced against the shortest exposure time $T_e = T_1$ used for the first acquired image. Each acquired n^{th} image is subjected to a specific v_p selection criteria for image reconstruction so that the new v_p values used for HDR image processing are between v_{max} and v_{min}. During camera calibration, one makes sure that the T_1 value is such that the brightest known test target produces a v_p value called v_B that satisfies $\mathbf{v_B \le v_{max}}$. In a similar vein, the final n^{th} image (n=N, an integer) is taken with the longest exposure time $\mathbf{T_N = P_N\ T_1}$ with $P_N \le P_{max}$ and where one makes sure during camera calibration that the P_N value is such that the weakest known test target for the designed HDR_D value produces a v_p value called v_w that meets the condition $\mathbf{v_w \ge v_{min}}$. This condition is also met when P_N is such that the exposure time based total scaled irradiance translation of the CRF satisfies $\mathbf{20log\ P_N = HDR_D - LDR_E}$. If $v_w < v_{min}$, the experimental light source illuminating the test target must be brightened further so $\mathbf{v_w \ge v_{min}}$.

Thus P_N and hence T_N are computed and experimentally verified to meet the specified HDR_D value. If experimentally one does not recover the deployed HDR_D value image, one must reduce the required HDR_D value until P_{max} is identified. Such criterion for camera calibration assures that all acquired images with different exposures starting from T_1 to T_N provide proposed technique needed v_p data that importantly falls in the experimentally measured sub-linear CRF regime. Using this select v_p data that is next mapped to I_s values using the experimental CRF, the unweighted image fusion (summation) of multiple exposure image set is used to produce the desired low contrast HDR image.

Depending on the selected v_B and v_w values, consecutive images can be designed to overlap a bit in target DR values to introduce some redundancy in the process. In this case, a given pixel where multiple I_s values are provided (and should be close in value given the linear CRF selection), an average of these redundant I_s values should be used to give the final I_s value for the pixel. The other N-2 T_n values (i.e., n not equal to 1 and N) are chosen to provide the scaled irradiance N-1 exposure controlled translations of maximum LDR_E dB per translation on the CRF to cover the full HDR_D range. If solving $M \times LDR_E = HDR_D$ gives an M that is not a whole integer, the last exposure will be a scaled input irradiance translation that is less than LDR_E. After the first image capture, int(M)-1=N-2 irradiance translations, each of LDR_E value are required. This in-turn implies that the exposure time with reference

to T_1 increases between intermediate images starting from the 2nd image by a factor equal to $\Delta P = 20 \log LDR_E$. The last n=Nth image undergoes a scaled input irradiance translation on the CRF of HDR_D – int(M) x LDR_E= HDR_D – (N-2)LDR_E. For example, with HDR_D=140 dB, LDR_E=60 dB, N=3, M=2.33, int(M)=2,

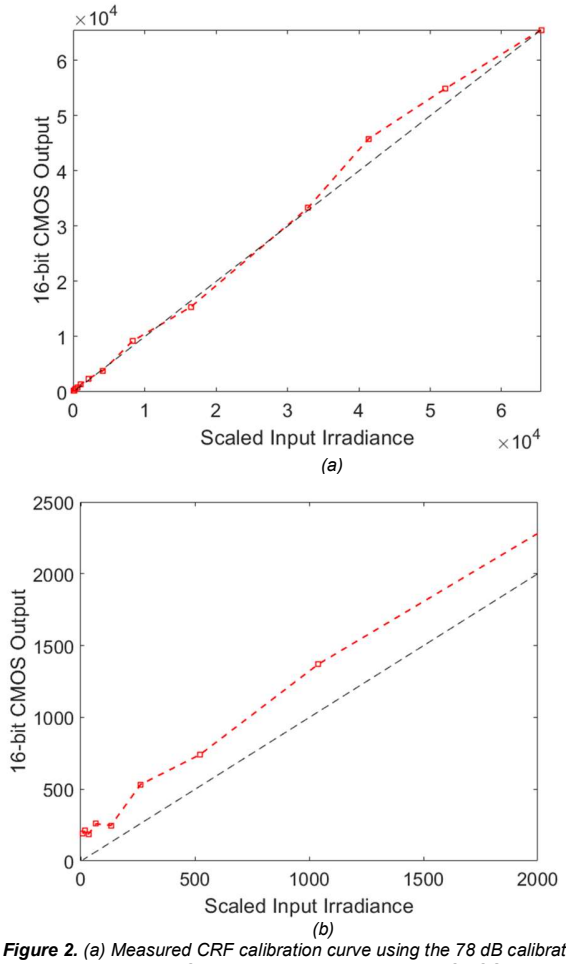

Figure 2. *(a) Measured CRF calibration curve using the 78 dB calibration target. (b) Zoomed in CRF curve shows the non-linear CMOS sensor response for low light levels with scaled input irradiance values under 250. The CRF curve's linear approximation has a sensor output offset d of ~ 200.*

$20 \log P_N$=140 – 60 gives $P_3=T_3/T_1= 10^4$. $P_2= T_2/T_1=10^3$ and last image translation is of 20 dB.

5. Measurement robustness is set by choice of v_{min} and v_W values that ensure all signal data within HDR_D limit provides an adequate Signal-to-Noise Ratio (SNR) (e.g., SNR > 2) for the experimental measurements. Both v_{min} and v_W should be set keeping in mind the $v_P=v_N$ values for dark light noise regions (i.e., Black region of test target) observed during the calibration and multi-exposure image testing process.

The concluded section has described the key steps needed to implement the proposed calibration empowered multi-exposure image processing technique that allows a non-linear CRF sensor to be used for extraction of multiple linear CRF regime LDR images that undergo minimalistic computations and allow the recovery of a true scaled irradiance low contrast HDR image, generally considered a challenging task. Note that during the calibration

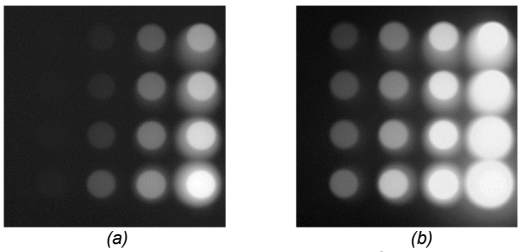

Figure 3. *Target Figure 1(b) sensor acquired images for exposure (a) T_1 and (b) T_2.*

process, HDR_D recovery range chosen has to be low enough to keep I_i and T_e within experimentally identified limits to preserve linear operations of the camera multi-exposure image sequence operations.

Experimental Verification

Figure 1(a) shows the design of the 78 dB HDR target used in CRF calibration required for the proposed multi-image HDR technique. Figure 1(b) is another design target (i.e., with different patch irradiance values) used to test the proposed multi-image technique. Both targets are designed for low contrast detection (i.e., 6 dB and under irradiance steps in the 16 patches) and are illuminated by a 60 Kilo-Lux visually bright setting Image Engineering (Germany) white LED powered light box. The monochrome CMOS sensor used is Thorlabs Quantalux S2100-M with 5 μm pixel pitch, 2.1 Mpixels and specified up-to 87 dB HDR rating with a 16-bit (i.e., 1 to 65,536 levels) v_p output. A 6 cm focal length imaging lens L1 is used to capture the target placed 105 cm from L1 and 6.4 cm from the sensor. Details on targets, optical set-up and CMOS sensor CRF calibration are described in ref.28 [28].

The essence of the CRF experimental generation process is to capture a single image just under saturation when observing the designed low contrast HDR test target. This image after computational processing for 25 ms provides the measured CMOS output v_p values for the known test patch HDR data, allowing one to plot a CRF curve (see Figure 2) and find a near slope 1 region in the CRF. The measured CRF is nonlinear for low input light levels as partly shown in the CRF zoomed view in Figure 2(b). Experiments described in detail in ref.28 confirm this non-linear behaviour of the deployed CMOS sensor and data shows that low contrast image recovery is not possible in the low light region over a 60 dB to near 90 dB level where 0 dB is the brightest pixel.

For the HDR_D=78 dB Figure 1(a) calibration target, a curve fit done on the Figure 2(a) data between 250 and 45,000 CMOS sensor v_p output reading connected to two specific target patches gives a slope nearest to 1, i.e., m=1.06 with ± 4.6% upper/lower bound with 95% confidence. Given this linear LDR CRF data, chosen are v_{min}=250 and v_{max}=40,000 giving an experimental linear LDR_E of 44 dB. To improve LDR linearity, note that a slightly lower v_{max} of 40,000 is chosen. N=2 images satisfies N x $LDR_E \geq HDR_D$ condition given LDR_E=44 dB and HDR_D=78 dB. For a T_1=0.207 ms, the brightest patch gives a v_B=34040 which satisfies the condition $v_B<v_{max}$, placing the brightest light within the measured linear CRF region. The measured v_n=113 for image 1 giving a worst case SNR=250/113= 2.2 where the weakest signal v_p used for image recovery is v_{min}=250. Given HDR_D-LDR_E= 78 – 44= 34 dB, P is computed to be 50, making $T_2=50T_1$=10.34 ms. Using the T_2 exposure setting, the second image is captured that gives a measured v_w=481 and a v_N=156 giving a worst case SNR=481/156= 3.1. Each target patch is fully recovered by a 100 x 100 = 10,000 CMOS

Table 1: N=2 images and Fig.1(b) target HDR recovery & comparison with Mann and Picard [14], Debevec and Malik [15], Mitsunaga and Nayar [16], and Robertson, Borman, & Stevenson [17], and Oh, Lee, Tai, and Kweon method [21].

Design (dB)	Riza and Ashraf	[14]	[15]	[16]	[17]	[21]
0	0	0	0	0	0	0
8	7.2	12.8	13.4	8.9	26.6	7.2
14	14.2	21.9	20.2	15.6	30.7	14.2
20	22.1	26.7	24	21.9	31.6	21.7
26	26.8	27.9	24.9	25.2	31.7	26.1
32	33	28.9	25.9	29.5	32.3	32.9
36	35.1	30.2	27.2	31.6	33.6	35.8
40	40.8	34.5	31.7	37.4	37.9	43.2
44	43.2	36.7	33.9	39.9	40.1	46.1
50	50.1	45.7	43.2	53.4	49.1	44.3
56	55.6	51.3	48.8	59.7	54.7	49.2
60	60.4	56.1	53.4	60.4	59.5	52.7
64	63.7	59.4	56.4	60.5	62.8	54.8
68	66.8	62.4	59.2	60.5	65.8	56.6
74	69.7	65.3	61.6	60.5	68.7	58.2
78	77.4	73.1	67.4	60.5	76.3	61.4

sensor pixels region with each image containing 1920 x 1080 pixels. Signal scaled irradiance data over the known 16 patch regions is computed using an average of these 10,000 pixel readings. Noise readings are taken in the no light (i.e., no target patch) region at the periphery of the acquired image. For the experiment, T_1+T_2=0.207+10.34= 10.547 ms, keeping image acquisition times within real-time video rates. Using a PC, image processing and image reconstruction takes 0.259 seconds. Figure 3 (a) and Figure 3 (b) using a log conversion of scaled irradiance data show the captured image 1 (using T_1) and image 2 (using T_2), respectively. The proposed technique based target scaled irradiances recovered are compared with prior art leading multi-exposure image processing LDR-to-HDR recovery methods [14-17, 21].

Specifically, in the Mann and Picard method [14], each pixel measured scaled irradiance in an acquired image is first weighted by the slope of the CRF at its specific irradiance level. Then the processed N im ages are summed such that all pixel specific scaled irradiance from all the images are added and the final scaled pixel irradiance is the average of these scaled irradiances. Debevec and Malik [15] use a hat function to weight each each pixel's measured scaled irradiance in an acquired image. This hat function can be written as:

$$w(z) = \begin{cases} z - Z_{min} \; for \; z \leq \frac{1}{2}(Z_{min} + Z_{max}) \\ Z_{max} - z \; for \; z > \frac{1}{2}(Z_{min} + Z_{max}) \end{cases}, \quad (1)$$

Table 2: N=2 images and modified target HDR recovery and comparison with [14-17], and [21].

Design (dB)	Riza and Ashraf	[14]	[15]	[16]	[17]	[21]
0	0	0	0	0	0	0
4	3.1	5.6	5.8	4.1	13.2	3.1
8	7.2	12.8	13.2	8.9	24.9	7.2
14	14.7	22.5	20.8	16.1	30.5	14.7
18	17.1	24.5	22.5	18.2	30.9	17
22	22.6	27.2	24.3	22.4	31.3	22.2
28	29.2	28.5	25.4	27	31.6	28.6
32	33.9	29.5	26.6	30.5	32.4	34.1
36	35.1	30.3	27.3	31.8	33.2	35.9
40	39.7	33.8	30.9	36.5	36.6	42.1
44	43.6	37.2	34.4	40.5	40.1	46.7
52	52.3	48.1	45.7	57.7	51	48.9
58	58.8	54.7	52	60.6	57.6	53.4
64	63.4	59.2	56.3	60.7	62.1	56.2
70	67.5	63.3	60	60.7	66.2	58.3
78	75.7	71.6	66.5	60.7	74.3	61.5

where Z_{min}, and Z_{max} are lowest and highest possible pixel values, respectively. For the deployed CMOS sensor, these values are 0 and 65535 for Z_{min}, and Z_{max} , respectively. Note that the hat function w(z) pixel weighting is applied in the logarithmic domain, i.e., the weighting is applied to the natural logarithm of each pixel's measured scaled irradiance. The final scaled pixel irradiance is the inverse logarithm of the weighted average of these scaled irradiances. A look at the hat function highlights the fact that this weighting method gives linearly less importance to pixel values at the extremes of the sensor output range while giving most weightage to pixel values in the mid-range of the detected sensor output signal.

For the Mitsunaga and Nayar method [16], each pixel measured scaled irradiance in an acquired image is first weighted by its SNR which is given by the ratio of the CRF and the CRF derivative, i.e., CRF′ at the specified irradiance level. In other words, pixel weight = CRF/CRF′. The final scaled pixel irradiance is the average of these scaled irradiances. In effect, pixel values with higher SNR get higher weightage.

Robertson, Borman, & Stevenson [17] use weights similar to Debevec and Malik coupled with the exposure time. They use a Gaussian-like function given as:

$$w(z) = exp\left[-W \cdot \frac{(z-Z_{mid})^2}{(Z_{mid})^2}\right] \quad (2)$$

The Gaussian function is scaled and shifted so that w(0) = w(Z_{max}) = 0 and w(Z_{mid}) = 1 where Z_{max}, and Z_{mid} are highest possible pixel value and the middle pixel value, respectively. For the camera used in this paper, the values were 65535 and 32768 for the Z_{max} and Z_{mid}, respectively. W is a numerical value that represents the confidence

Table 3: N=2 images and modifed target HDR recovery & comparison with [14-17] and [21] when the overall target illumination is reduced by a factor of 2.

Design (dB)	Riza and Ashraf	[14]	[15]	[16]	[17]	[21]
0	0	0	0	0	0	0
4	3.2	5.1	4.9	3.4	5.7	3.2
8	7.4	11.4	10.9	7.6	9.9	7.4
14	15.3	20.5	17.4	14.4	12.1	14.8
18	18.1	22.4	19	16.4	12.4	16.9
22	24.2	25.3	20.7	20.8	12.8	22.3
28	30.1	26.6	21.7	25.3	13.1	28.7
32	33.9	27.5	22.7	28.6	13.8	33.9
36	35	28.2	23.4	29.8	14.5	35.6
40	39.6	31.6	26.8	34.4	17.8	41.8
44	43.5	35	30.3	38.5	21.3	46.4
52	52.2	45.9	41.6	55.7	32.2	50.7
58	58.7	52.4	47.9	58.6	38.7	54.9
64	63.2	56.9	52.2	58.8	43.2	57.3
70	67.3	61	55.8	58.8	47.2	59.1
78	75.4	69	62.2	58.8	55.2	61.7

in the reliability of pixel observations at the extremes. Each pixel's measured scaled irradiance in an acquired image is first weighted by the computed Gaussian function and then multiplied by the exposure time of the respective image. Then the processed weighted N images are summed so the final scaled pixel irradiance is the average of all the weighted scaled irradiances. Clearly this method gives higher weight to images with longer exposure times u sed to recover lower light levels. For the Oh, Lee, Tai, and Kweon method [21], a rank minimization algorithm is demonstrated using a synthesized multi-exposure LDR image data set used to recover the HDR image. This matrix rank minimization-based method requires the photo-sensor to be linear over its full operating dynamic range so one can computationally approach an ideal rank-1 structure that results when combining multi-exposure LDR images. Hence this technique is inherently limiting given its usage with certain near ideal linear lower dynamic range sensors.

For a true comparison, the prior-art methods deploy our full HDR CRF data set acquired during the single image acquisition calibration process with Figure 1(a) designed target with 16 scaled irradiance values to cover the full HDR of 78 dB and with low contrast irradiance step inter-patch settings. The computed recovered target patch scaled irradiance values are shown in Table 1. Note that Ref. 17 deployed W values of 4 and 16, where W=16 was used for CMOS outputs that are very noisy at both extremes. Using the Figure 2 and Figure 3 experimental data, scaled irradiance computations for the Robertson, Borman, & Stevenson method are done using W=1, W=4 and W=16. Note that using W=1 and W=16 give worse results compared to the W=4 results, hence Table 1 lists the W=4 results. Given the challenge of LDR to HDR low contrast image recovery using a limited linearity "realistic" optical CMOS sensor, Table 1 results indicate the higher accuracy and reliability of the proposed multi-exposure technique over leading prior-art multi-exposure HDR generation methods. As expected, the ref.21 technique works for a limited 44 dB LDR where the deployed camera has a linear CRF. Table 2 shows imaging results obtained using another 78 dB HDR test target with mostly different designed scaled irradiances for the 16 patches. Again, the measured data shows the superior performance of the proposed multi-exposure LDR to HDR recovery technique over the cited prior art methods. It is also important to note that when the overall illuminating incident light level changes by a factor β, the T_e for the acquired images is also scaled linearly by $1/\beta$ without changing other camera settings determined during camera calibration. β can be measured by an independent light meter point sensor mounted on the camera.

Using the modified target used in Table 2 and using a 30 Kilolux target illumination versus the calibration illumination setting of 60 Kilolux, i.e., β=0.5, the exposure times relative to prior experiments are doubled as $1/\beta$=2, Table 3 experimental data (when compared to Table 2) indeed shows that the modified target scaled irradiances have again been recovered despite the illumination level falling by a factor of 2. The proposed multi-exposure HDR image low contrast recovery accuracy is mainly limited by the measured slope variation of the experimental CMOS sensor within the identified and deployed linear CRF region. An ideal sensor would have no variation in slope m, the existence of which is practically unreal. Experiments show a P_{max}=50 for a 78 dB HDR robust image recovery with an illumination range from 200 Kilolux to 7.5 Kilolux using T_2 of 3.29 ms and 78.66 ms, respectively. Recovery beyond 78 dB HDR_D starts to become untrue for P_n>50 where multi-exposure operations become non-linear. In addition, with P_n fixed at 50, recovery beyond 78 dB HDR_D starts to become untrue when illumination light level goes below 7.5 Kilolux where CMOS sensor low light level detection operations become non-linear. Minimum specified T_e for the CMOS sensor is 0.030 ms. For 78 dB HDR_D recovery with an illumination range from 200 Kilolux to 7.5 Kilolux, T_1 used is 0.059 ms and 1.57 ms, respectively. Because of the dynamic range overlap region between image 1 and image 2 v_p data due to the chosen v_w and v_B operational settings, a minimum P_n=30 is also accurately able to recover the full 78 dB target patch scaled irradiance values, implying a moderately shorter T_2 can also be deployed for HDR recovery. In other words, depending on the chosen v_w and v_B operational settings, P_n has a range of operations such that $P_{min} \leq P_n \leq P_{max}$. For the demonstrated experiment, P_{min}=30 and P_{max}=50 and use of a higher P_n such as P_n=100 makes the weakest target patch 78 dB HDR recovery inaccurate as the higher P_n value drives the camera system into its non-linear operational regime.

Conclusion

For the first time, proposed and successfully experimentally demonstrated is a calibration empowered minimalistic computational operations method based on measured v_p and P_n limits to recover an HDR low contrast image using multiple exposure image processing and a limited linearity response optical image sensor. Experiments using calibrated test targets demonstrate 78 dB HDR low contrast (6 dB irradiance step across HDR) image recovery with the proposed technique using 2 multi-exposure linear 44 dB LDR images that shows higher accuracy and reliability results

when compared with leading prior-art methods. The proposed technique can be used in the CAOS smart camera [29] that includes a CMOS-mode that provides high spatial resolution low light scene intelligence for operation of the extreme linear dynamic range CAOS-mode for smart image fusion-based image recovery. Future work involves testing the proposed method with real scenes.

Acknowledgement: The authors thank PhD student Mohsin A. Mazhar for experimental data support.

References

[1] J. J. McCann and A. Rizzi, The Art and Science of HDR Imaging. vol. 26, John Wiley & Sons, 2012.

[2] E. Reinhard, G. Ward, S. Pattanaik, and P. Debevec, High Dynamic Range Imaging: Acquisition, Display, and Image-based Lighting, Elsevier Morgan Kaufmann Publisher, 2005.

[3] L. C. P. Gouveia and B. Choubey. "Advances on CMOS image sensors," Sensor Review, vol. 36. no.3, pp. 231-239, 2016.

[4] A. Spivak, A. Belenky, A. Fish, and O. Yadid-Pecht, "Wide-dynamic-range CMOS image sensors—comparative performance analysis," IEEE Transactions on Electron Devices, vol. 56, no. 11 pp. 2446-2461, 2009.

[5] S. Kavadias, B. Dierickx, D. Scheffer, A. Alaerts, D. Uwaerts, and J. Bogaerts, "A logarithmic response CMOS image sensor with on-chip calibration," IEEE Journal of Solid-state circuits vol. 35, no. 8, pp. 1146-1152, 2000.

[6] C. W. Wyckoff, "An experimental extended exposure response film," SPIE Newsletter, pp. 16–20, 1962.

[7] S. Ochi and S. Yamanaka, "Solid state image pickup device," US Patent, 4,541,016, (filed 1982) 1985.

[8] P. J. Burt, "The pyramid as a structure for efficient computation," in Multiresolution image processing and analysis, pp. 6-35. Springer, Berlin, Heidelberg, 1984.

[9] L. Alston, D. Levinstone, W. Plummer, "Exposure Control System for an Electronic Imaging Camera Having Increased Dynamic Range," US Patent 4,647,975, (filed 1985) 1987.

[10] S. Mann, "Compositing Multiple Pictures of the Same Scene," Proc. IS & T 46th Annual Meeting, pp.50-52, 1993.

[11] P. J. Burt and R. J. Kolczynski, "Enhanced image capture through fusion," Proc. 4th IEEE Int. Conf. Comput. Vis., 1993,

[12] M. Mase, S. Kawahito, M. Sasaki, Y. Wakamori, and M. Furuta, "A wide dynamic range CMOS image sensor with multiple exposure-time signal outputs and 12-bit column-parallel cyclic A/D converters," IEEE Journal of Solid-State Circuits, vol. 40, no. 12, pp. 2787–2795, 2005.

[13] O. Yadid-Pecht and E. Fossum, "Wide intrascene dynamic range CMOS APS using dual sampling," IEEE Transactions on Electron Devices, vol. 44, no. 10, pp. 1721–1723, 1997.

[14] S. Mann and R. Picard, "On Being 'Undigital' with Digital Cameras: Extending Dynamic Range by Combining Different Exposed Pictures," Proc. IS & T 48th Annual Meeting, pp. 442–448, 1995.

[15] P. Debevec and J. Malik, "Recovering High Dynamic Range Radiance Maps from Photographs," ACM SIGGRAPH ' 97, pp.369–378, 1997.

[16] T. Mitsunaga and S. K. Nayar. "Radiometric Self Calibration," Proc. of CVPR, vol. 2, pp. 374–380, 1999.

[17] M. A. Robertson, S. Borman, and R. L. Stevenson, "Dynamic range improvement through multiple exposures," Int. Conf. Image Process., 3, 159–163, 1999.

[18] A. A. Goshtasby, "Fusion of multi-exposure images," Image Vis. Comput., vol. 23, no. 6, pp. 611–618, 2005.

[19] T. Mertens, J. Kautz, and F. Van Reeth, "Exposure fusion: A simple and practical alternative to high dynamic range photography," Comput. Graph. Forum, vol. 28, no. 1, pp. 161–171, 2009

[20] C. Lee, Y. Li, and V. Monga, "Ghost-free high dynamic range imaging via rank minimization," IEEE Signal Process. Lett., vol. 21, no. 9, pp. 1045–1049, 2014.

[21] T-H Oh, J-Y Lee, Y-W Tai, and I. S. Kweon, "Robust high dynamic range imaging by rank minimization," IEEE Transactions on Pattern Analysis and Machine Intelligence, vol. 37, no. 6, pp. 1219-1232, 2015.

[22] Y. Tsin, V. Ramesh, T. Kanade, "Statistical Calibration of the CCD Imaging Process," Proc. Int'l Conf. Computer Vision, vol. 1, pp. 480-487, 2001.

[23] D. Grossberg and S. K. Nayar, "Determining the camera response from images: What is knowable?," IEEE Trans. Pattern Anal. Mach. Intell., vol. 25, no. 11, pp. 1455–1467, 2003.

[24] M. D. Grossberg and S. K. Nayar, "Modeling the space of camera response functions," IEEE Trans. Pattern Anal. Mach. Intell., vol. 26, no.10, pp.1272-1282, 2004.

[25] J.-Y. Lee, Y. Matsushita, B. Shi, I. S. Kweon, and K. Ikeuchi, "Radiometric calibration by rank minimization," IEEE Trans. Pattern Anal. Mach. Intell., vol. 35, no. 1, pp. 144–156, 2013.

[26] Y.C. Chang and J.F. Reid, "RGB Calibration for Color Image-Analysis in Machine Vision," IEEE Trans. Image Processing, vol. 5, no. 10, pp. 1414-1422, 1996.

[27] 2:1 (or 6 dB) Contrast Patch Target Pairs-based HDR Contrast Resolution Chart, Imatest LLC, Boulder, USA.

[28] N. A. Riza and M. A. Mazhar, " Robust Low Contrast Image Recovery over 90 dB Scene Linear Dynamic Range using CAOS Camera," paper in the IS & T 2020 Electronic Imaging Conference Proc., Burlingame, California, USA, Jan.26-30, 2020.

[29] N. A. Riza and M. A. Mazhar, "177 dB Linear Dynamic Range Pixels of Interest DSLR CAOS Camera," IEEE Photonics Journal, vol. 11, no. 2, 2019

Author Biography

Nabeel A. Riza holds Masters (1985) & Ph.D. (1989) degrees in electrical engineering from Caltech. Since 2011, he holds the Chair Professorship in Electrical & Electronic Engineering at University College Cork, Ireland. His awards include the 2019 IS&T/OSA Edwin H. Land Medal, 2018 IET Achievement Medal, and 2001 ICO Prize. He is a Fellow of the US NAI, IEEE, OSA, EOS, SPIE, and Honorary Fellow Engineers Ireland Society. His research focus is applied optics and photonics.

Nazim Ashraf holds a Ph.D. degree in computer science from University of Central Florida. He is a postdoctoral scholar under supervision by Prof. Nabeel Riza at the Photonics Information Processing Systems Lab., University College Cork, Ireland. He is currently on leave as Associate Professor from Forman Christian College (A Chartered University), Lahore.

JOIN US AT THE NEXT EI!

IS&T International Symposium on

Electronic Imaging

SCIENCE AND TECHNOLOGY

Imaging across applications . . . Where industry and academia meet!

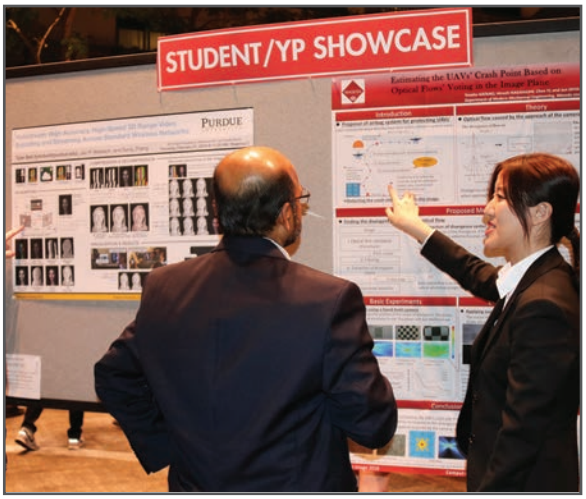

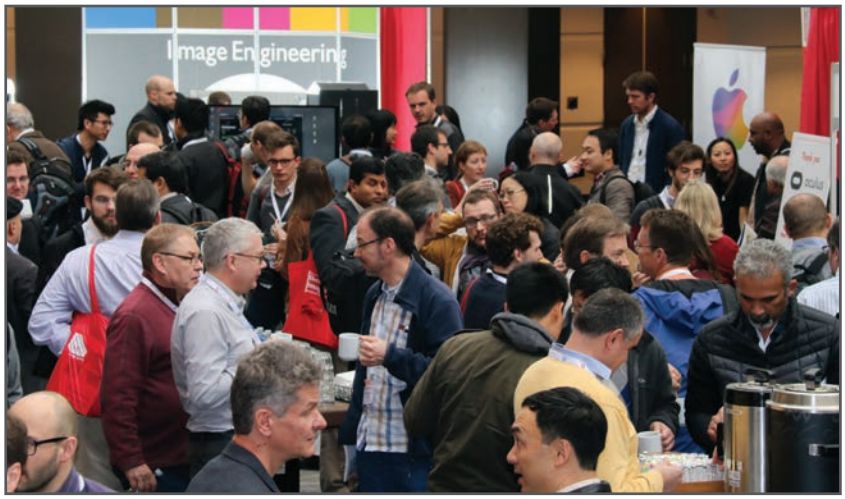

• SHORT COURSES • EXHIBITS • DEMONSTRATION SESSION • PLENARY TALKS •
• INTERACTIVE PAPER SESSION • SPECIAL EVENTS • TECHNICAL SESSIONS •

www.electronicimaging.org

IS&T
imaging.org